THE JOURNAL OF PHYSICAL CHEMISTRY Letters

Letter

Cite This: J. Phys. Chem. Lett. 2018, 9, 3511−3516

pubs.acs.org/JPCL

Charge Environment and Hydrogen Bond Dynamics in Binary Ionic Liquid Mixtures: A Computational Study

Nikhil V. S. Avula, Anirban Mondal,† and Sundaram Balasubramanian*

Chemistry and Physics of Materials Unit, Jawaharlal Nehru Centre for Advanced Scientific Research, Bangalore 560064, India

Supporting Information

ABSTRACT: The extent of charge transfer between the cation and the anion in a room-temperature ionic liquid depends on the basicity of the anion. Ion charges determined in the condensed state via density functional theory calculations capture this effect rather well, and charges derived in such a manner have been employed in force field-based molecular dynamics simulations to quantitatively reproduce several physical properties of the liquids. However, the issue of transferability of cation charges in mixtures of ionic liquids, say with one type of cation and two different anion types needs to be addressed. Herein, we demonstrate that the cation charge in such a mixture varies linearly with anion composition, a result that ties in rather well with X-ray photoelectron spectroscopic experiments. The variation in cation charge with bulk anion composition is shown to be a result of changes in its coordination environment. Cations surrounded by a higher proportion of more basic anions possess lower charges than those surrounded by less basic anions. Time scales for the exchange of anion types for the occupation of hydrogen bonding sites around the cation have been determined and are seen to be constituted by three processes—breakage of existing hydrogen bond, diffusion to the hydrogen bonding site and displacement of the incumbent anion from its site in the cation coordination shell. These time scales explain the differences observed between infrared and NMR spectroscopic experiments in ionic liquid mixtures rather well.

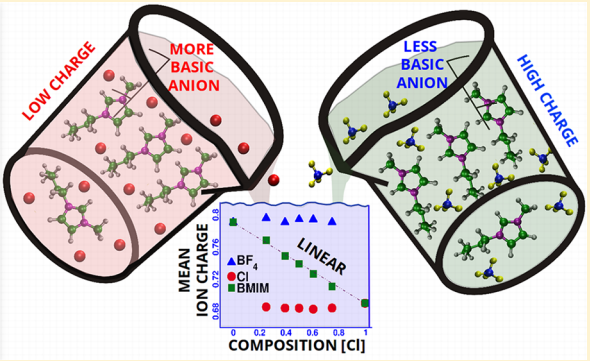

Room temperature ionic liquids (RTILs) offer a wide choice of properties for their use as either solvents or electrolytes by allowing for the possibility of mixing different ionic components.[1−3] However, the compositional space of ILs is too large to be explored by experiments alone. Computer simulations play an essential role complementing experiments as well as offering insights into the microscopic behavior of ILs.[4−7]

In this regard, empirical force field (FF)-based molecular dynamics (MD) simulations are apt, as they can offer microscopic insights as well as provide estimates of bulk/interfacial properties while using a modest amount of computational resource.[8−12] However, the reliability of MD simulations is contingent upon the fidelity of the force field.[13−15] Researchers have recognized the need to take into account charge transfer and polarizability effects between the ions in the condensed phase, for a quantitative comparison between the modeled system and experiment.[16,17] A crucial outcome of interion charge transfer is the reduction in their formal charges from unity.[18] Polarizable force fields account for these phenomena explicitly, and hence are more "physical" than nonpolarizable ones. However, this additional detail often comes at an increased computational cost.[19,20]

Although nonpolarizable force fields do not account for polarization explicitly, fixed partial charges, if chosen appropriately, can capture the effects of ion polarization in a mean field manner.[21] Studies have shown that some structural (like X-ray structure factor)[22,23] and dynamical properties (like diffusion constants)[24] are most affected by the choice of partial charges, hence it is imperative that they are parametrized consistently.

As the extent of charge transfer between the cation and the anion can depend on their type, a nonpolarizable force field based on fixed ion charges (subunity) will need to be transferable to mixtures, i.e., ionic liquids which contain one type of cation and two different types of anions (say). Addressing this problem, using periodic quantum density functional theory (DFT) calculations, we demonstrate the linear variation of cation charge with anion composition, a result that segues with results from X-ray photoelectron spectroscopy (XPS). This observation constitutes the basis on which a linear charge mixing approach can be adopted within a force field. MD simulations, using such a force field, reproduce experimental data on IL mixtures and shed considerable light on the microscopic exchange mechanisms of anion types in the coordination shell of a cation. These studies are pursued in a binary ionic liquid (BIL) system with 1-butyl-3-methylimidazolium [BMIM] as the common cation and chloride [Cl] and tetrafluoroborate [BF_4] as the counteranions (see section I of the Supporting Information).[25]

Received: May 10, 2018
Accepted: June 8, 2018
Published: June 8, 2018

DOI: 10.1021/acs.jpclett.8b01481
J. Phys. Chem. Lett. 2018, 9, 3511−3516

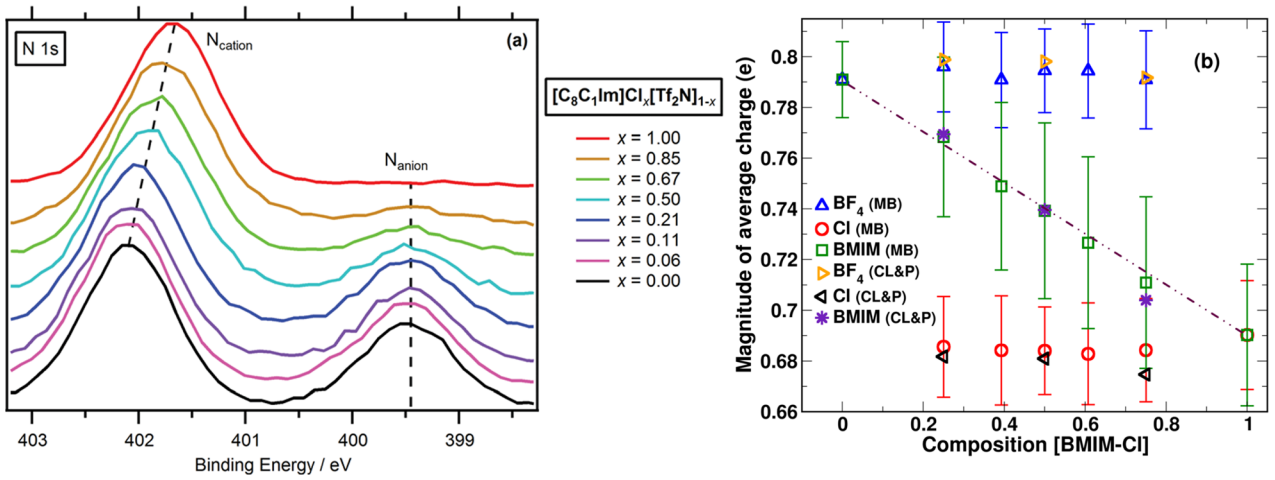

Figure 1. (a) High-resolution N 1s XPS spectra of $[OMIM][Cl]_x[NTf_2]_{1-x}$ mixture at different compositions, taken from the work of Licence et al.[28] and (b) magnitude of average net ion charges (NICs) of BMIM, [Cl] and $[BF_4]$ ions vs composition obtained from simulations. The labels indicate the ions and the corresponding force fields used to derive the NICs: (i) MB force field[31,33] and (ii) CL&P force field[34−38] (see Supporting Information for additional details). Magenta dash-dot line is drawn as a guide to the eye.

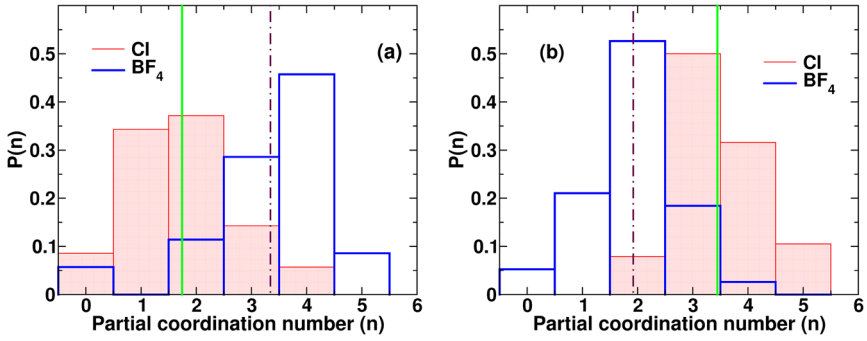

Figure 2. Probability density vs partial coordination number of (a) high charge cations (charge greater than +0.78e) and (b) low charge cations (charge less than +0.70e), in a BIL with 50:50 composition. The green vertical line indicates the average partial [Cl] coordination number (average number of [Cl] ions surrounding a cation), and the maroon dash-dot line represents the average partial $[BF_4]$ coordination number.

The condensed phase electronic charge density was estimated by DFT calculations of a representative set of snapshots of each BIL mixture. These snapshots were selected from classical MD trajectories of BILs generated from two different force fields. Details of these calculations are presented in the Supporting Information. The electron density was used to calculate the atomic site charges using the *DDEC/c3* method[26,27] and the net ionic charge (NIC) was obtained as the sum of atomic site charges of all atoms of an ion. Figure 1b shows the variation of average NIC of [BMIM], [Cl] and $[BF_4]$ ions with respect to composition of the BIL mixture. The average NIC of cations varies linearly between the values of the pure components, irrespective of the force field employed. By contrast, the average NICs of both the anions remain unchanged with composition. Recently, Licence et al. investigated the charge environment of ions in IL mixtures using N 1s X-ray photoelectron spectroscopy.[28] Figure 1a shows the N 1s XP spectra of $[OMIM][Cl]_x[NTf_2]_{1-x}$ system, which contains nitrogen in both the cation as well as in the $[NTf_2]$ anion. The XPS measurements revealed that the binding energy of nitrogen atom in cation varied "quasi-linearly" with anion composition whereas that in the $[NTf_2]$ anion remained unchanged. Moreover, the binding energies of all the carbon and nitrogen atoms in the cation varied quasi-linearly. Various studies have shown that the cation charge is largely centered on the ring and is independent of the alkyl tail length.[29−31] In general, the XPS binding energies of most atoms (including carbon and nitrogen) are linearly correlated to the partial charge on the atoms.[32] This would mean that the atomic partial charges of cation atoms, derived from XPS binding energies, would also vary quasi-linearly with composition. This observation serves as a direct experimental evidence to the linear variation of NIC obtained in our simulations.

In order to understand the origin of the linear trend of cation charge with anion mole fraction, we examined the local environment of cations in the BIL at 50:50 anion composition. The average NIC of cation at this composition is +0.74e. We first selected two sets of cations—low charge (NIC values less than +0.70e) and high charge (NIC values greater than +0.78e) cations. We then estimated the partial coordination number for cations belonging to each of these two sets separately.

Figure 2 shows the probability density of a cation (in the 50:50 mixture) to have a certain coordination number of [Cl] and $[BF_4]$ anions. The average number (shown as green vertical line) of [Cl] ions in the first coordination shell of a cation is higher for the low charge cations and lower for a cation with high charge. More the number of chloride ions surrounding a cation, more is the extent of charge transfer and hence lower is that cation's NIC. This analysis clearly shows that the NIC of a cation is affected by both the number and composition of the

DOI: 10.1021/acs.jpclett.8b01481
J. Phys. Chem. Lett. 2018, 9, 3511−3516

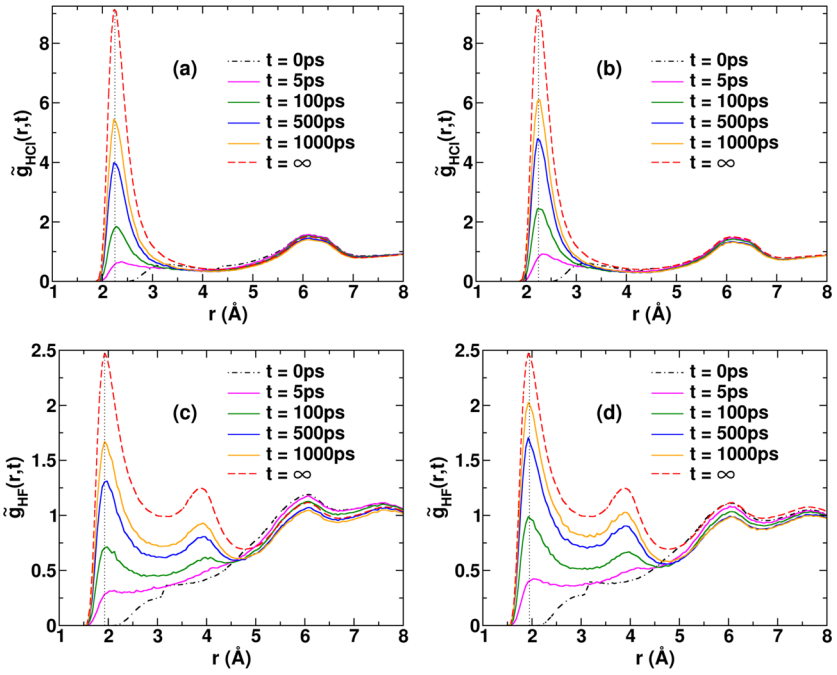

Figure 3. Time evolution of (a) $\tilde{g}_{HCl}(r,t)$ from the population of cations initially hydrogen bonded to [Cl] ions, (b) $\tilde{g}_{HCl}(r,t)$ from the population of cations initially hydrogen bonded to $[BF_4]$ ions, (c) $\tilde{g}_{HF}(r,t)$ from the population of cations initially hydrogen bonded to [Cl] ions and (d) $\tilde{g}_{HF}(r,t)$ from the population of cations initially hydrogen bonded to $[BF_4]$ ions. 50:50 BIL mixture was used for this analysis. The maroon dotted line indicates the position of the first peak at $t = \infty$ (equilibrium).

anions surrounding it. This correlation can be used to rationalize the linear trends in average NIC of cation (Figure 1). The average NIC of cations depends on the composition of their first solvation shell and which in turn depends on the bulk composition of the mixture (assuming homogeneous mixing; see ref 39). These results encouraged us to adopt a linear charge mixing scheme for the ion charges modeled via classical MD simulations. While the charges of the anions are chosen to be independent of the anion composition of the IL, that of the cation is chosen as the weighted sum of the charges of the cations used in the pure systems—the weight being the mole fraction of the individual anions present in the mixture. In a liquid modeled with a polarizable force field or one with a fluctuating charge model, the charge on a specific cation would be dependent on its environment. The linear charge mixing scheme employed by us here can be viewed as a mean field approximation to such models which include explicit polarizability.[20]

To gauge the efficacy of the linear charge mixing rule, we have also simulated the $[BMIM][NTf_2]_x[SCN]_{1-x}$ liquid, for which experimental density data was available. Simulated densities are found to be in good agreement with experimental values having at most 2% error (Figure S3). Both simulated and experimental desities show a linear trend indicating the mixture to be ideal, consistent with most IL mixtures.[40]

Hydrogen bonds play a vital role in influencing the bulk properties of ILs, including shear viscosity.[41,42] Among the many hydrogen bonding sites on the imidazolium cation, the H_A atom (see Figure S1) forms the strongest hydrogen bond with the donor atoms (X) on anions.[43,44] Hence, for the sake of simplicity, we consider only H_A–X hydrogen bonds. Spectroscopic studies and MD simulations of IL mixtures have shown that H_A–X hydrogen bonds switch from one anion to another as the cation rotates within its solvation shell.[45,46] Doseok et al. investigated the nature of hydrogen bonds in liquid [BMIM]-$[Cl]_x[BF_4]_{1-x}$ using IR and NMR spectroscopy.[45] While the former showed two *distinct* peaks (C_R–H vibrational modes) corresponding to each type of H_A–X hydrogen bonds, the H_A proton NMR chemical shift showed a single peak whose value exhibited a monotonic change with anion composition. They attributed this conflicting result to the different time scales probed by the two spectroscopic methods: subpicosecond ($\approx$ 0.1 ps) for IR and millisecond ($\approx$ 0.6 ms) for NMR. They conclude that the hydrogen bond switching time scale is higher than the IR time scale and lower than the NMR time scale (0.1 ps $< \tau <$ 0.6 ms).

We now employ our force field within the linear charge mixing framework to study the microscopic structure and dynamics of $[BMIM][Cl]_x[BF_4]_{1-x}$ IL mixtures. Note that although the chloride end of the cation NIC in Figure 1B terminates at a value of +0.69e, the MB force field[31,33] parametrized the cation NIC in the pure dialkylimidazolium chloride IL to be +0.64e. Hence the linear charge mixing is performed with the terminal values prescribed by the MB force field for the pure IL systems. In particular, we focus on the dynamics of the hydrogen bond between the most acidic ring hydrogen H_A and the donor atom of anion, X = Cl,F. H_A–X pair correlation functions (Figure S6) and spatial distribution functions (Figure S5) show that [Cl] ions have a marginally higher propensity of forming a hydrogen bond when compared to $[BF_4]$ ions, consistent with experiments on similar IL mixtures.[46] The cation reorientational time correlation functions and the cation–anion hydrogen bond time correlation functions (Figure S11–12) indicate that the H_A–Cl hydrogen bond lasts longer than the H_A–F bond (see Supporting Information). These results are consistent with the fact that [Cl] ions interact stronger with the cations than $[BF_4]$ ions do.

In order to understand these spectroscopic observations, we obtain the time scales of hydrogen bond (HB) switching in

DOI: 10.1021/acs.jpclett.8b01481
J. Phys. Chem. Lett. 2018, 9, 3511–3516

pure and mixed ionic liquids. We define a time dependent pair correlation function $\tilde{g}_{HX}(r,t)$ (defined below), between the most acidic hydrogen (H_A) of the cation and the donor atom (X = Cl,F) of the anion.

$$\tilde{g}_{HX}(r,t) = \frac{V}{\tilde{N}_X 4\pi r^2}\left\langle \frac{1}{\tilde{N}_H(t_0)}\sum_{i=1}^{\tilde{N}_H}\sum_{j=1}^{\tilde{N}_X}\delta \times (r - |\vec{r}_j^{\,X}(t_0+t) - \vec{r}_i^{\,H}(t_0+t)|)\right\rangle \quad (1)$$

$$\tilde{g}_{HX}(r,t) = \frac{V}{\tilde{N}_X 4\pi r^2 dr}\left\langle \frac{\tilde{n}_{HX}(r, t_0+t)}{\tilde{N}_H(t_0)}\right\rangle \quad (2)$$

where V is the volume of the simulation box, $\tilde{N}_X$ is the number of *selected* donor atoms, $\tilde{N}_H(t_0)$ is the number of H_A atoms belonging to *selected* cations at time t_0, δ represents the Dirac delta function, $\vec{r}$ represents the position of atoms, and $\langle\ \rangle$ represents the average over time origin t_0. In the case of HB switching between the same kind of anion (say [Cl] to [Cl]), $\tilde{N}_X = N_X - 1$, N_X being the total number of X type donor atoms, because the anion hydrogen bonded to cation at time $t = 0$ is not considered in the calculation of $\tilde{g}_{HX}(r,t)$, whereas, in the case of HB switching between different anion types (say [Cl] to [F]), $\tilde{N}_X = N_X$. Equation 2 gives a simplified version of $\tilde{g}_{HX}(r,t)$, where $\tilde{n}_{HX}(r,t_0 + t)$ is the number of X atoms (in case of like anion switching, we exclude the X atom hydrogen bonded to selected cation at t_0) situated at a distance between r and $r + dr$ from the *selected* H_A atoms. At time t_0, we select cations which are hydrogen bonded to only one of the two anion types in the mixture. This selected population of cations represents an out of equilibrium scenario where only one type of hydrogen bonding is present. Hence, this population would relax to the equilibrium hydrogen bonding statistics by process of anion exchange. The anion that hydrogen bonds with the cation at any time t can be of the same type as the one that the cation was hydrogen bonded to at time t_0, or it could be of another type. Thus, it is possible to calculate from the MD trajectory at a given composition, four different $\tilde{g}(r,t)$. $\tilde{g}_{HX}(r,t)$ tells us the time evolution of this anion exchange process (see Figure 3).

In all the $\tilde{g}_{HX}(r,t)$ plots, we see that the first peak, which is absent at time t_0 increases in intensity with time. This indicates that other anions (i.e., ones which were not initially hydrogen bonded to the selected cations) start replacing the original anions which were hydrogen bonded to the cation initially. To obtain a quantitative estimate of this relaxation process, we compute the radial coordination number $\tilde{c}_{HX}(t)$. The coordination number is calculated by integrating $\tilde{g}_{HX}(r,t)$ up to the first solvation shell cutoff. Equation 3 gives a normalized function $f(t)$, which can be used to compare the time scales of different kinds of anion exchange.

$$f(t) = \frac{\tilde{c}_{HX}(t) - \tilde{c}^0_{HX}}{\tilde{c}^\infty_{HX} - \tilde{c}^0_{HX}} \quad (3)$$

where $\tilde{c}^0_{HX}$ is the coordination number at time t_0 and $\tilde{c}^\infty_{HX}$ is the coordination number when the system is in equilibrium ($t = \infty$). Figure 4 shows the function $f(t)$ for all kinds of anion exchange in the 50:50 BIL mixture as well as in the pure ionic liquid systems.

Time-constants of the relaxation process, listed in Table 1, were obtained from fitting $f(t)$ to a sum of three exponential

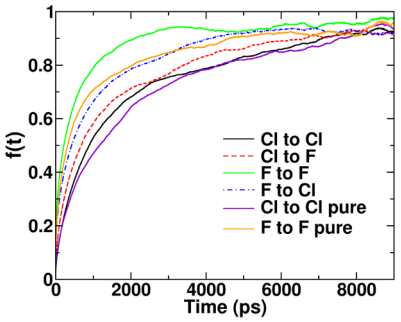

Figure 4. Normalized function $f(t)$ of all kinds of anion exchange in mixed as well as pure ionic liquid systems. Read the labels as "A to B" to mean $f(t)$ of A type anions with respect to cations that were hydrogen bonded to B type anions at time t_0. The labels with suffix "pure" refers to neat IL systems.

decay functions (see Supporting Information). The migration of [Cl] ions to the occupied hydrogen bonding sites are the slowest processes, while the migration of [BF_4] ions to the occupied hydrogen bonding sites are the fastest. We also note that the migration of [Cl] ions to sites occupied by [BF_4] anions (τ = 1.9 ns) is *slower* compared to the migration of [BF_4] ions to [Cl] (τ = 1.5 ns) occupied hydrogen bonding sites. This might seem counterintuitive, as [Cl] ion forms a stronger hydrogen bond with the cation and hence is more likely to replace [BF_4] ions than vice versa. Such an argument might be valid if the [Cl] ions were freely available in the liquid, ready to displace [BF_4] ions from hydrogen bonded sites. However, [Cl] ions are already hydrogen bonded to other sites (either to a different cation or to other ring hydrogens). Thus, we propose a simple, mechanical picture of this anion exchange as a three step process: first, the incoming anion has to break its hydrogen bond and become a free ion (Step I), followed by its relative diffusion to the hydrogen bonding location (Step II) and finally, to displace the incumbent anion (Step III). The relative hydrogen bond lifetime of H_A–Cl, estimated from the continuous hydrogen bond time correlation function is greater than that of H_A–F (see Table S7). Hence [Cl] ions are slower in step I than the [BF_4] ions. Thus, in the case of [Cl] ions, Step I is the rate limiting step, and hence they are slow to replace [BF_4] ions than vice versa.

From this study, we estimate the characteristic time scale of the hydrogen bond switching phenomenon to be on the order of nanoseconds (1.4–2.7 ns). IR spectroscopy, which probes the system at subpicosecond time scale, essentially captures a static hydrogen bond network and hence detects two distinct C_R–H_A vibrational peaks corresponding to two different H_A–X bond types. However, NMR spectroscopy, probing larger time scales, captures a dynamic hydrogen bond network and thus exhibits a single chemical shift value.[45]

In sum, we have shown that the average charge of cation in a binary ionic liquid mixture containing two different anion types displays a linear trend as a function of anion composition. This observation is supported by the linear trend in the experimentally observed XPS binding energies of cation atoms with composition.[28] We have found that the charge of a specific cation is directly correlated to the composition of its first coordination shell: the greater the fraction of more basic anions, the lower the cation charge. The agreement of our findings with experiments gives credence to our framework to obtain condensed phase site charges. We propose a linear charge mixing scheme to obtain the atomic site charges for MD

DOI: 10.1021/acs.jpclett.8b01481
J. Phys. Chem. Lett. 2018, 9, 3511–3516

Table 1. Parameters of Fit of $f(t)$ to a Sum of Three Exponential Functions

relaxation process	A_1	τ_1 (ps)	A_2	τ_2 (ps)	A_3	τ_3 (ps)	$\langle\tau\rangle$ (ps)
[Cl] to [Cl]	0.102	13	0.629	975	0.270	7892	2745
[Cl] to [BF_4]	0.102	9	0.472	523	0.426	3984	1919
[BF_4] to [Cl]	0.190	7	0.480	526	0.331	3894	1542
[BF_4] to [BF_4]	0.226	7	0.612	489	0.122	9393	1449

simulations of BIL mixtures. MD simulations performed within such an approach were used to study the switching of cation hydrogen bond between anions. The hydrogen bond switching is shown to be a three-step process involving hydrogen bond breaking, relative diffusion, and hydrogen bond forming, respectively. The time scales of each of these processes have been determined which rationalize the differences in experimental results of IR and NMR spectroscopies.

■ ASSOCIATED CONTENT

Supporting Information

The Supporting Information is available free of charge on the ACS Publications website at DOI: 10.1021/acs.jpclett.8b01481.

System details, computational details, pair correlation functions, spatial distribution functions, MSDs, and hydrogen bond time correlation functions (PDF)

Archived file containing CP2K input files for geometry optimization and cube file generation, LAMMPS input, parameter and data files for NVT simulations (ZIP)

■ AUTHOR INFORMATION

Corresponding Author

*E-mail: bala@jncasr.ac.in Phone: +91 (80) 2208 2808. Fax: +91 (80) 2208 2766.

ORCID

Sundaram Balasubramanian: 0000-0002-3355-6764

Present Address

†Max Planck Institute for Polymer Research, Mainz, Germany

Notes

The authors declare no competing financial interest.

■ ACKNOWLEDGMENTS

We thank DST for support.

■ REFERENCES

(1) Brennecke, J. F.; Maginn, E. J. Ionic Liquids:Innovative Fluids for Chemical Processing. *AIChE J.* **2001**, *47*, 2384−2389.

(2) Armand, M.; Endres, F.; MacFarlane, D. R.; Ohno, H.; Scrosati, B. Ionic-liquid materials for the electrochemical challenges of the future. *Nat. Mater.* **2009**, *8*, 621−629.

(3) MacFarlane, D. R.; Tachikawa, N.; Forsyth, M.; Pringle, J. M.; Howlett, P. C.; Elliott, G. D.; Davis, J. H.; Watanabe, M.; Simon, P.; Angell, C. A. Energy applications of ionic liquids. *Energy Environ. Sci.* **2014**, *7*, 232−250.

(4) Hu, Z.; Margulis, C. J. Heterogeneity in a room-temperature ionic liquid: Persistent local environments and the red-edge effect. *Proc. Natl. Acad. Sci. U. S. A.* **2006**, *103*, 831−836.

(5) Bhargava, B. L.; Balasubramanian, S. Refined potential model for atomistic simulations of ionic liquid [bmim][PF_6]. *J. Chem. Phys.* **2007**, *127*, 114510.

(6) Weingärtner, H. Understanding ionic liquids at the molecular level: Facts, problems, and controversies. *Angew. Chem., Int. Ed.* **2008**, *47*, 654−670.

(7) Rumble, C. A.; Kaintz, A.; Yadav, S. K.; Conway, B.; Araque, J. C.; Baker, G. A.; Margulis, C.; Maroncelli, M. Rotational Dynamics in Ionic Liquids from NMR Relaxation Experiments and Simulations: Benzene and 1-Ethyl-3-Methylimidazolium. *J. Phys. Chem. B* **2016**, *120*, 9450−9467.

(8) Canongia Lopes, J. N.; Pádua, A. A. Nanostructural organization in ionic liquids. *J. Phys. Chem. B* **2006**, *110*, 3330−3335.

(9) Zhao, W.; Leroy, F.; Heggen, B.; Zahn, S.; Kirchner, B.; Balasubramanian, S.; Müller-Plathe, F. Are There Stable Ion-Pairs in Room-Temperature Ionic Liquids? Molecular Dynamics Simulations of 1-n-Butyl-3-methylimidazolium Hexafluorophosphate. *J. Am. Chem. Soc.* **2009**, *131*, 15825−15833.

(10) Bedrov, D.; Vatamanu, J.; Hu, Z. Ionic liquids at charged surfaces: Insight from molecular simulations. *J. Non-Cryst. Solids* **2015**, *407*, 339−348.

(11) He, Y.; Qiao, R.; Vatamanu, J.; Borodin, O.; Bedrov, D.; Huang, J.; Sumpter, B. G. Importance of Ion Packing on the Dynamics of Ionic Liquids during Micropore Charging. *J. Phys. Chem. Lett.* **2016**, *7*, 36−42.

(12) Bruce, D. W.; Cabry, C. P.; Lopes, J. N.; Costen, M. L.; D'Andrea, L.; Grillo, I.; Marshall, B. C.; McKendrick, K. G.; Minton, T. K.; Purcell, S. M.; et al. Nanosegregation and Structuring in the Bulk and at the Surface of Ionic-Liquid Mixtures. *J. Phys. Chem. B* **2017**, *121*, 6002−6020.

(13) Morrow, T. I.; Maginn, E. J. Molecular Dynamics Study of the Ionic Liquid 1-n-Butyl-3-methylimidazolium Hexafluorophosphate. *J. Phys. Chem. B* **2002**, *106*, 12807−12813.

(14) Bagno, A.; D'Amico, F.; Saielli, G. Computer simulation of diffusion coefficients of the room-temperature ionic liquid [bmim]-[BF_4]: Problems with classical simulation techniques. *J. Mol. Liq.* **2007**, *131*−*132*, 17−23.

(15) Dommert, F.; Schmidt, J.; Qiao, B.; Zhao, Y.; Krekeler, C.; Delle Site, L.; Berger, R.; Holm, C. A comparative study of two classical force fields on statics and dynamics of [EMIM][BF_4] investigated via molecular dynamics simulations. *J. Chem. Phys.* **2008**, *129*, 224501.

(16) Dommert, F.; Wendler, K.; Berger, R.; Delle Site, L.; Holm, C. Force fields for studying the structure and dynamics of ionic liquids: A critical review of recent developments. *ChemPhysChem* **2012**, *13*, 1625−1637.

(17) Chaban, V. V.; Prezhdo, O. V. Polarization versus Temperature in Pyridinium Ionic Liquids. *J. Phys. Chem. B* **2014**, *118*, 13940−13945.

(18) Schmidt, J.; Krekeler, C.; Dommert, F.; Zhao, Y.; Berger, R.; Site, L. D.; Holm, C. Ionic charge reduction and atomic partial charges from first-principles calculations of 1,3-dimethylimidazolium chloride. *J. Phys. Chem. B* **2010**, *114*, 6150−6155.

(19) Son, C. Y.; McDaniel, J. G.; Schmidt, J. R.; Cui, Q.; Yethiraj, A. First-Principles United Atom Force Field for the Ionic Liquid $BMIM^+BF_4^-$: An Alternative to Charge Scaling. *J. Phys. Chem. B* **2016**, *120*, 3560−3568.

(20) Uhlig, F.; Zeman, J.; Smiatek, J.; Holm, C. First-Principles Parametrization of Polarizable Coarse-Grained Force Fields for Ionic Liquids. *J. Chem. Theory Comput.* **2018**, *14*, 1471−1486.

(21) Schröder, C. Comparing reduced partial charge models with polarizable simulations of ionic liquids. *Phys. Chem. Chem. Phys.* **2012**, *14*, 3089.

(22) Campetella, M.; Gontrani, L.; Bodo, E.; Ceccacci, F.; Marincola, F. C.; Caminiti, R. Conformational isomerisms and nano-aggregation in substituted alkylammonium nitrates ionic liquids: An x-ray and computational study of 2-methoxyethylammonium nitrate. *J. Chem. Phys.* **2013**, *138*, 184506.

(23) Campetella, M.; Gontrani, L.; Leonelli, F.; Bencivenni, L.; Caminiti, R. Two Different Models to Predict Ionic-Liquid Diffraction

DOI: 10.1021/acs.jpclett.8b01481
J. Phys. Chem. Lett. 2018, 9, 3511−3516

Patterns: Fixed-Charge versus Polarizable Potentials. *ChemPhysChem* **2015**, *16*, 197−203.
(24) Youngs, T. G. A.; Hardacre, C. Application of Static Charge Transfer within an Ionic-Liquid Force Field and Its Effect on Structure and Dynamics. *ChemPhysChem* **2008**, *9*, 1548−1558.
(25) (a) [BMIM][Cl] melts at 339K (see ref 25b), thus our simulations of this system are in supercooled liquid state. Despite that, these anions were chosen as (i) they are common and (ii) exhibit the largest total ion charge difference in the respective pure ILs. (b) Holbrey, J. D.; Reichert, W. M.; Nieuwenhuyzen, M.; Johnson, S.; Seddon, K. R.; Rogers, R. D. Crystal polymorphism in 1-butyl-3-methylimidazolium halides: supporting ionic liquid formation by inhibition of crystallization. *Chem. Commun.* **2003**, 1636−1637.
(26) Manz, T. A.; Sholl, D. S. Chemically meaningful atomic charges that reproduce the electrostatic potential in periodic and nonperiodic materials. *J. Chem. Theory Comput.* **2010**, *6*, 2455−2468.
(27) Manz, T. A.; Sholl, D. S. Improved atoms-in-molecule charge partitioning functional for simultaneously reproducing the electrostatic potential and chemical states in periodic and nonperiodic materials. *J. Chem. Theory Comput.* **2012**, *8*, 2844−2867.
(28) Villar-Garcia, I. J.; Lovelock, K. R. J.; Men, S.; Licence, P. Tuning the electronic environment of cations and anions using ionic liquid mixtures. *Chem. Sci.* **2014**, *5*, 2573−2579.
(29) Hunt, P. A.; Kirchner, B.; Welton, T. Characterising the electronic structure of ionic liquids: An examination of the 1-butyl-3-methylimidazolium chloride ion pair. *Chem. - Eur. J.* **2006**, *12*, 6762−6775.
(30) Kohagen, M.; Brehm, M.; Thar, J.; Zhao, W.; Müller-Plathe, F.; Kirchner, B. Performance of Quantum Chemically Derived Charges and Persistence of Ion Cages in Ionic Liquids. A Molecular Dynamics Simulations Study of 1- n -Butyl-3-methylimidazolium Bromide. *J. Phys. Chem. B* **2011**, *115*, 693−702.
(31) Mondal, A.; Balasubramanian, S. Quantitative prediction of physical properties of imidazolium based room temperature ionic liquids through determination of condensed phase site charges: A refined force field. *J. Phys. Chem. B* **2014**, *118*, 3409−3422.
(32) Sundberg, P.; Larsson, R.; Folkesson, B. On the core electron binding energy of carbon and the effective charge of the carbon atom. *J. Electron Spectrosc. Relat. Phenom.* **1988**, *46*, 19−29.
(33) Mondal, A.; Balasubramanian, S. A Refined All-Atom Potential for Imidazolium-Based Room Temperature Ionic Liquids: Acetate, Dicyanamide, and Thiocyanate Anions. *J. Phys. Chem. B* **2015**, *119*, 11041−11051.
(34) Canongia Lopes, J. N.; Deschamps, J.; Pádua, A. A. Modeling Ionic Liquids Using a Systematic All-Atom Force Field. *J. Phys. Chem. B* **2004**, *108*, 2038−2047.
(35) Canongia Lopes, J. N.; Deschamps, J.; Pádua, A. A. Corrections-Modeling Ionic Liquids Using a Systematic All-Atom Force Field. *J. Phys. Chem. B* **2004**, *108*, 2038−2047.
(36) Canongia Lopes, J. N.; Pádua, A. A. Molecular force field for ionic liquids composed of triflate or bistriflylimide anions. *J. Phys. Chem. B* **2004**, *108*, 16893−16898.
(37) Canongia Lopes, J. N.; Pádua, A. A. Molecular force field for ionic liquids III: Imidazolium, pyridinium, and phosphonium cations; chloride, bromide, and dicyanamide anions. *J. Phys. Chem. B* **2006**, *110*, 19586−19592.
(38) Canongia Lopes, J. N.; Pádua, A. A.; Shimizu, K. Molecular force field for ionic liquids IV: Trialkylimidazolium and alkoxycarbonyl-imidazolium cations; alkylsulfonate and alkylsulfate anions. *J. Phys. Chem. B* **2008**, *112*, 5039−5046.
(39) Payal, R. S.; Balasubramanian, S. Homogenous mixing of ionic liquids: molecular dynamics simulations. *Phys. Chem. Chem. Phys.* **2013**, *15*, 21077−210833.
(40) Clough, M. T.; Crick, C. R.; Grasvik, J.; Hunt, P. A.; Niedermeyer, H.; Welton, T.; Whitaker, O. P. A physicochemical investigation of ionic liquid mixtures. *Chem. Sci.* **2015**, *6*, 1101−1114.
(41) Hunt, P. A. Why does a reduction in hydrogen bonding lead to an increase in viscosity for the 1-butyl-2,3-dimethyl-imidazolium-based ionic liquids? *J. Phys. Chem. B* **2007**, *111*, 4844−4853.
(42) Gehrke, S.; von Domaros, M.; Clark, R.; Holloczki, O.; Brehm, M.; Welton, T.; Luzar, A.; Kirchner, B. Structure and lifetimes in ionic liquids and their mixtures. *Faraday Discuss.* **2018**, *206*, 219−245.
(43) Thar, J.; Brehm, M.; Seitsonen, A. P.; Kirchner, B. Unexpected hydrogen bond dynamics in imidazolium-based ionic liquids. *J. Phys. Chem. B* **2009**, *113*, 15129−15132.
(44) Skarmoutsos, I.; Welton, T.; Hunt, P. A. The importance of timescale for hydrogen bonding in imidazolium chloride ionic liquids. *Phys. Chem. Chem. Phys.* **2014**, *16*, 3675−3685.
(45) Cha, S.; Kim, D. Anion exchange in ionic liquid mixtures. *Phys. Chem. Chem. Phys.* **2015**, *17*, 29786−29792.
(46) Matthews, R. P.; Villar-Garcia, I. J.; Weber, C. C.; Griffith, J.; Cameron, F.; Hallett, J. P.; Hunt, P. A.; Welton, T. A structural investigation of ionic liquid mixtures. *Phys. Chem. Chem. Phys.* **2016**, *18*, 8608−8624.

DOI: 10.1021/acs.jpclett.8b01481
J. Phys. Chem. Lett. 2018, 9, 3511−3516